Constitutive Endocytosis and Degradation of the Pre-T Cell Receptor

Maddalena Panigada,[1] Simona Porcellini,[1] Eliane Barbier,[2] Sonja Hoeflinger,[4] Pierre-André Cazenave,[2,3] Hua Gu,[6] Hamid Band,[5] Harald von Boehmer,[4] and Fabio Grassi[4]

[1]*Dipartimento di Biologia e Genetica per le Scienze Mediche, Università degli Studi di Milano, 20133 Milano, Italy*
[2]*Département d'Immunologie, Institut Pasteur, 75724 Paris Cedex 15, France*
[3]*Université Pierre et Marie Curie (Paris 6), 75005 Paris, France*
[4]*Department of Pathology, Dana Farber Cancer Institute and* [5]*Lymphocyte Biology Section, Division of Rheumatology, Immunology and Allergy, Brigham and Women's Hospital, Harvard Medical School, Boston, MA 02115*
[6]*Laboratory of Immunology, National Institute of Allergy and Infectious Diseases, National Institutes of Health, Rockville, MD 20852*

Abstract

The pre-T cell receptor (TCR) signals constitutively in the absence of putative ligands on thymic stroma and signal transduction correlates with translocation of the pre-TCR into glycolipid-enriched microdomains (rafts) in the plasma membrane. Here, we show that the pre-TCR is constitutively routed to lysosomes after reaching the cell surface. The cell-autonomous down-regulation of the pre-TCR requires activation of the src-like kinase $p56^{lck}$, actin polymerization, and dynamin. Constitutive signaling and degradation represents a feature of the pre-TCR because the γδTCR expressed in the same cell line does not exhibit these features. This is also evident by the observation that the protein adaptor/ubiquitin ligase c-Cbl is phosphorylated and selectively translocated into rafts in pre-TCR– but not γδTCR-expressing cells. A role of c-Cbl–mediated ubiquitination in pre-TCR degradation is supported by the reduction of degradation through pharmacological inhibition of the proteasome and through a dominant-negative c-Cbl ubiquitin ligase as well as by increased pre-TCR surface expression on immature thymocytes in c-Cbl–deficient mice. The pre-TCR internalization contributes significantly to the low surface level of the receptor on developing T cells, and may in fact be a requirement for optimal pre-TCR function.

Key words: c-Cbl • pre-TCR • T cell development • thymocyte • ubiquitin

Introduction

The pre-TCR is composed of the disulfide-linked TCRβ/pre-TCRα (pTα)* heterodimer in noncovalent association with CD3 signal-transducing modules (1). The CD3γ and CD3ε chains as well as the disulfide linked ζ–ζ homodimer were shown to play crucial roles in proximal signal transduction by the pre-TCR (2–6), whereas the CD3δ chain was shown to be associated with the pre-TCR (1) but dispensable for its function (7, 8). Deletion of essential pre-TCR–CD3 complex components induces a severe thymic atrophy with a block at the G_0/G_1 phase of the cell cycle of $CD25^+44^-$ $CD4^-8^-$ double negative (DN) 3 cells and arrest of αβ T cells at DN stage of thymocyte development. Few $CD4^+8^+$ double positive (DP) cells were detected in pTα and ζ chain–deficient mice (4–6, 9, 10) and both pTα and ζ chains were required for the allelic exclusion of the TCRβ locus (11, 12). These observations demonstrate that the expression of the pre-TCR–CD3 complex by immature DN thymocyte regulates the development of the αβ T cell lineage by ensuring efficient TCRβ selection with proper transition to the DP stage. In addition to these roles

The online version of this article contains supplemental material.

Address correspondence to Fabio Grassi, Dana Farber Cancer Institute, 1 Jimmy Fund Way, Boston, MA 02115. Phone: 617-632-6885; Fax: 617-632-6881; E-mail: fabio_grassi@dfci.harvard.edu

*Abbreviations used in this paper: DN, double negative; DP, double positive; ER, endoplasmic reticulum; EGFP, enhanced green fluorescent protein; FTOC, fetal thymic organ culture; HA, hemagglutinin; HRP, horseradish peroxidase; LAMP, lysosomal-associated membrane protein; PDI, protein disulfide isomerase; pTα, pre-T cell receptor α; TRITC, tetramethylrhodamine isothiocyanate.

 J. Exp. Med. © The Rockefeller University Press • 0022-1007/2002/06/1585/13 $5.00
Volume 195, Number 12, June 17, 2002 1585–1597
http://www.jem.org/cgi/doi/10.1084/jem.20020047

in T cell development, pre-TCR expression was recently shown to be crucially involved in the development of leukemia/lymphoma in Notch transgenic mice (13, 14).

Observations in transgenic mice expressing a TCRβ chain with an attached endoplasmic reticulum (ER) retrieval signal clearly indicated that the exit of the pre-TCR from the ER/*cis*-Golgi apparatus is required for the development of the αβ T cell lineage (15). Mice expressing a truncated pre-TCR devoid of the extracellular portion displayed efficient developmental progression, which suggested that the pre-TCR functions independently of an exogenous ligand (16). The biochemical demonstration of cell-autonomous translocation of the pre-TCR complex into glycolipid-enriched membrane domains (rafts) and cell-autonomous signaling supported this hypothesis, thus defining differences in initiation of signaling between the pre-TCR on the one hand and the αβTCR and γδTCR on the other hand, the latter two requiring ligation to observe similar biochemical alterations (17).

Endocytosis and molecular sorting of receptors are mainly regulated by dileucine- and tyrosine-based motifs present in the cytoplasmic tails that act as coated pit localization signals (18, 19). The dileucine-based motif identified in the CD3γ chain (20) can bind clathrin-coated vesicle adaptor proteins in vitro and mediate endocytosis of the TCR upon activation of protein kinase C (21). After protein kinase C–mediated internalization, the TCR is recycled back to the cell surface upon CD3γ dephosphorylation (22). In contrast, antigenic stimulation and activation of the $p56^{lck}$ tyrosine kinase targets cell surface TCRs for lysosomal degradation (23, 24). In resting cells, the TCR is constitutively internalized and recycled back to the cell surface. TCR ligation prevents recycling and initiates the degradation of the TCR–CD3 complex (25). The recent demonstration that ubiquitin carries an endocytosis signal (26, 27) and can target the degradation of monoubiquitinated proteins leads to the hypothesis that CD3 and ζ chains that are ubiquitinated after αβTCR engagement could play a role in targeting activated TCR–CD3 complexes for lysosomal degradation. Indeed, most ubiquitinated plasma membrane receptors are targeted for lysosomal degradation (28, 29). The ubiquitination and internalization of several growth factor receptors depend on the ubiquitin ligase activity of the product of the protooncogene *c-cbl* (30–33), which is phosphorylated after αβTCR stimulation (34).

The cell-autonomous signaling by the pre-TCR poses the question of whether the fate of the receptor resembles that of ligated TCRs and may, at least in part, be responsible for the low cell surface expression on developing thymocyte. Here, we show that in contrast to the αβTCR and γδTCR, the pre-TCR is constitutively routed to and degraded in lysosomes. The rapid turnover is blocked by sequestering monomeric actin, by the expression of a dominant-negative dynamin, and by the inhibition of $p56^{lck}$ activation. Moreover, the diminution of pre-TCR degradation by proteasome inhibitors and the inhibition of c-Cbl suggests that ubiquitination is involved in targeting the pre-TCR to the degradative pathway.

Materials and Methods

Antibodies, Cell Lines, Retroviral Vectors, and Mice. mAbs specific for the following antigens were used: protein disulfide isomerase (PDI; provided by G. Gatti, Department of Biological and Technological Research, University Hospital of San Raffaele [Dibit-HSR], Milan, Italy), β actin (A-5441; Sigma-Aldrich), giantin-CD107b (provided by H.P. Hauri, Biozentrum, Basel, Switzerland; reference 35), CD3ε (145-2C11), TCR Cβ (H57-597), TCR Vβ8 (F23.1), CD4 (GK1.5), CD8 (53-6.7), CD25 (PC61), CD44 (IM7; BD PharMingen), TCRδ (3A10; reference 36), ζ chain (G3; reference 37), and phosphotyrosine (4G10; Upstate Biotechnology). The following polyclonal immunoglobulins were used: anti-CD3ε (sc-1127), anti–c-Cbl (sc-170), anti-$p56^{lck}$ (sc-433; Santa Cruz Biotechnology, Inc.), and rabbit anti–ζ chain (provided by L. Samelson, National Cancer Institute, Bethesda, MD). For FACS® analysis of pre-TCR expression, cells were stained with biotinylated H57-597 mAb revealed by streptavidin–PBXL-3 (Martek). The SCID mice–derived thymocyte cell lines SCIET.27, SCB.29 (38), SCγδ.28, SCβ–enhanced green fluorescent protein (EGFP; reference 17), the T cell hybridoma B6.2.16 (38), and thymoma M14T (39) were used. In FACS® experiments, 10 μg/ml cycloheximide and 1 μM bafilomycin A1 were used. Cells were incubated with cycloheximide for 2 h, and a 1-h incubation with bafilomycin preceded the cell culture with the two drugs together. The EGFP-encoding bicistronic retroviral vector used in this study was derived by the matrix metalloproteinase vector (provided by J.-S. Lee, Harvard Medical School, Boston, MA; reference 40) and constructed by E. Jaeckel (Dana Farber Cancer Institute, Boston, MA). The plasmids encoding wild-type and K44A mutant dynamin (41) were obtained from M. Fabbri (Dibit-HSR, Milan, Italy). Plasmids for wild-type and mutant hemagglutinin (HA)-tagged c-Cbl were previously described (42). C-$Cbl^{-/-}$ C57BL/6 mice were used (43). Embryos from timed C57BL/6 pregnant female mice were used for fetal thymic organ culture (FTOC) and to obtain fetal thymocytes for microscopy. FTOC in the presence of vehicle (DMSO) or 10 μM PP2 (Calbiochem) was performed in IMDM, sodium pyruvate, 2-mercaptoethanol, L-glutamine, 20 mM Hepes, Nutridoma SP (Boehringer-Mannheim), 0.4% lipid-free BSA, and 8.1 μg/ml monothioglycerol.

Fluorescence Microscopy. After adhesion on poly-L-lysine–coated coverslip, SCβ-EGFP cells were fixed in 3% paraformaldehyde and permeabilized in PBS, 0.15% Triton X-100 for 5 min. In some experiments, cells were pretreated for 6 h with 0.5 μM bafilomycin A1 (Calbiochem) or with the vehicle of the drug (DMSO) as a control. After permeabilization, slides were incubated with the indicated antibodies followed by tetramethylrhodamine isothiocyanate (TRITC)–labeled secondary antibody. For staining with LysoTracker, cells were incubated in IMDM complete medium, 100 nM LysoTracker for 2 h at 37°C. After fixation and permeabilization, embryonic thymocytes were incubated with goat polyclonal anti–TCRβ immunoglobulins followed by a TRITC-labeled secondary antibody and then with antilysosomal-associated membrane protein (LAMP)-2 mAb followed by FITC-conjugated secondary antibody. The cells were visualized on an integrated DeltaVision system (Applied Precision) including an IX70 inverted microscope with a 60× objective (Olympus). Images were captured with a cooled, charge-coupled device camera (Princeton Instruments). 40–50 *z*-series optical sections were captured at 0.2-μm intervals, and out of focus light was removed by iterative deconvolution on an Octane 2 workstation (Silicon Graphics). Projections were generated with SoftwoRx software (Applied Precision).

Surface Labeling, Immunoprecipitation, and Electrophoresis. Cell surface biotinylation was performed as previously described (44). In brief, cells were washed in PBS and incubated in 1 ml PBS, 5 mM NHS-LC-biotin (Pierce Chemical Co.) for 1 h at 4°C. After washing in PBS, 20 mM glycine, the cells were lysed in 1% Brij 96 (Fluka) or 0.5% Triton X-100 (Bio-Rad Laboratories) and 60 mM N-octyl β-glucopyranoside (Sigma-Aldrich) lysis buffer. In proteasome inhibition experiments, cells were incubated with 200 nM epoxomicin (Boston Biochem) or vehicle (DMSO) as a control. Immunoprecipitations of pre-TCR–associated CD3ε chains were performed by dissociation of 1% Brij 96 TCRβ-specific immunocomplexes and reprecipitations with CD3ε-specific antibodies as previously described (45). Immunodepletion of pre-TCR–CD3 was achieved by three sequential immunoprecipitations of 1% Brij 96 cell lysates using F23.1 mAb at 20 μg/ml followed by protein A–Sepharose. For two-dimensional nonreducing versus reducing SDS-PAGE, immunoprecipitates were run in SDS sample buffer under nonreducing conditions in a discontinuous Laemmli SDS–polyacrylamide (5–15% gradient) gel. The first dimension strips were then equilibrated in reduced SDS sample buffer for 30 min at room temperature and then run into a second 5–15% gradient SDS-polyacrylamide gel. The gels were blotted onto nitrocellulose membrane (Amersham Pharmacia Biotech) probed with horseradish peroxidase (HRP)–conjugated avidin (Amersham Pharmacia Biotech), and then stripped and reprobed with anti-CD3ε antibodies revealed by HRP-conjugated secondary antibodies for normalization.

Cell Fractionation and Sucrose Gradients. After two washes in ice-cold PBS, cells were resuspended in hypotonic buffer (20 mM Tris-HCl, pH 7.5, 1 mM EGTA, 1 mM $MgCl_2$, 0.5 mM DTT, and protease inhibitors) and incubated for 10 min on ice. Cells were then disrupted by homogenization on ice with a dounce homogenizer. Salt concentration was adjusted to 150 mM NaCl, and intact cells, nuclei, and cytoskeleton were pelleted by centrifugation at 5,000 rpm for 5 min in microcentrifuge at 4°C. The low speed supernatant was centrifuged at 100,000 *g* for 60 min. The resulting pellet was considered the membrane fraction and the supernatant was considered the soluble proteins fraction. The pellet was lysed in Triton X-100/N-octyl β-glucopyranoside and equal amounts of proteins of the various fractions were loaded on gel. For sucrose gradient fractionations, cells were lysed in Triton X-100 as previously described (46) and equal amounts of solubilized proteins for the different samples were mixed with 1 ml 80% sucrose and overlaid with two phases of 2 ml 30% sucrose and 1 ml 5% sucrose, respectively. Samples were centrifuged at 200,000 *g* at 4°C for 14–16 h. Rafts fractions (from 3 to 5) as well as loading zone fractions (from 9 to 12) were pooled, resolved by SDS-PAGE in 8–15% gradient gels, transferred to nitrocellulose membranes, and blotted with anti–c-Cbl and anti-Lck immunoglobulins.

Online Supplemental Material. We provide the following as supplemental material: (a) images of multiple SCβ-EGFP cells stained with PDI, giantin antibodies, or incubated with LysoTracker showing the predominant localization of the pre-TCR in lysosomes; (b) an image showing the colocalization of TCRβ and CD3 in multiple SCβ-EGFP cells; (c) immunoprecipitation with TCRβ mAb of surface-labeled SCB.29 cells showing the reduction of pre-TCR turnover in cells treated with lactacystin; and (d) immunoblot analysis of SCB.29 cells with antiubiquitin rabbit serum showing the diminution of free ubiquitin upon proteasome inhibition with epoxomicin. Online supplemental figures are available at http://www.jem.org/cgi/content/full/jem.20020047/DC1.

Results

Constitutive Targeting of the Pre-TCR to Lysosomes. Transfection of the SCID thymocyte-derived cell line SCIET.27 with a rearranged TCRβ gene leads to expression of the pre-TCR in the plasma membrane (1). Microscopic analysis of SCIET.27 cells transfected with TCRβ-EGFP (SCβ-EGFP) revealed the accumulation of the green fluorescence in a vesicular intracellular compartment. The identity of such a compartment was investigated by staining with anti-PDI antibodies as a marker of ER, anti-giantin antibodies to label the Golgi apparatus, and LysoTracker, a red fluorescent dye that specifically accumulates in lysosomes. Fig. 1 shows the projections of multiple optical sections of selected cells in which the green fluorescence is exclusively colocalized with the lysosomal probe. Almost 60% of TCRβ-EGFP colocalized with the lysosomal marker on different 0.2-μm sections (Fig. 1, histogram and legend). Incubation of cells with cycloheximide blocking the de novo protein synthesis resulted in the diminution of green fluorescence in TCRβ-EGFP–expressing cells, but not in cells transfected with EGFP alone. However, the addition of bafilomycin A1, which blocks the acidification of endosomes, counteracted the effect of cycloheximide, suggesting that the diminution of fluorescence detected by cycloheximide treatment was the result of the selective lysosomal degradation of the TCRβ-EGFP fusion protein (Fig. 2 A). To rule out an artificial TCRβ-EGFP fusion protein–dependent routing of the pre-TCR to lysosomes, we analyzed pre-TCR–expressing thymocytes ex vivo. Microscopic analysis of day-15 embryonic thymocytes after permeabilization and intracellular staining with TCRβ and LAMP-2 antibodies revealed the colocalization of the two antibodies in TCRβ-expressing cells (Fig. 2 B), which indicates that the trafficking of the pre-TCR to lysosomes occurred in vivo as well as in TCRβ-EGFP–transfected cell lines (SCβ-EGFP). Intracellular staining of TCRβ-EGFP–transfected cells with CD3ε antibodies detected with TRITC-labeled anti-Ig revealed the colocalization of the two fluorochromes (Fig. 2 C), which suggests that pre-TCR–associated CD3ε chains were concomitantly targeted to lysosomes. This conclusion was supported by immunoblot analysis of CD3ε molecules after bafilomycin A1 treatment of the pre-TCR–expressing cell line SCB.29, which is derived from SCIET.27 by transfection with TCRβ (1). 6 h after treatment with the drug a twofold increase in CD3ε protein was detected. When the same analysis was performed with the parental untransfected SCIET.27 cell line or the γδTCR transfectants (SCγδ.28), bafilomycin A1 treatment had no effect on CD3ε levels, suggesting that the increase of CD3ε levels in SCB.29 cells was dependent on the association of CD3 with the pre-TCR (Fig. 2 D).

Limited Stability of the Pre-TCR in the Plasma Membrane. The apparent difference in signal initiation by the pre-TCR on one hand and the αβTCR or γδTCR on the other (16, 17) is consistent with the constitutive routing of the pre-TCR to lysosomes and the spontaneous

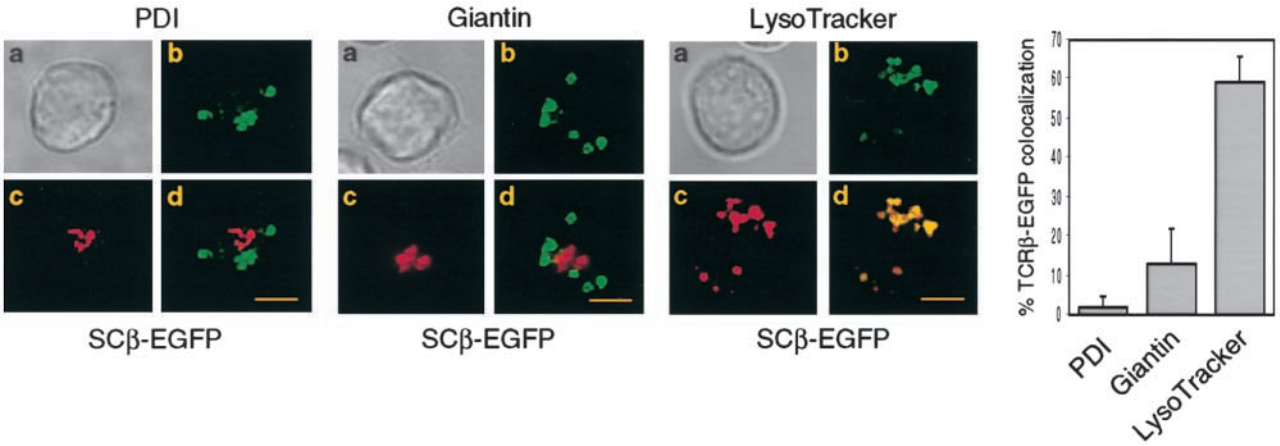

Figure 1. Localization of the pre-TCR in lysosomes. SCβ-EGFP cells were permeabilized and stained with the indicated antibodies or incubated with LysoTracker. (a) Phase-contrast image, (b) TCRβ-EGFP, (c) staining with the indicated reagent, and (d) merged images are shown. Images of multiple cells showing comparable patterns are provided as supplemental material (see Figure S1, A–C, available at http://www.jem.org/cgi/content/full/jem.20020047/DC1). 40–50 *z*-series optical sections were captured at 0.2-μm intervals and processed by a DeltaVision system (Materials and Methods). Bars, 10 μm. The histogram shows the percentage of TCRβ-EGFP colocalized with the indicated marker on single 0.2-μm sections. The obtained values were 1.72 ± 3.1% (n = 41) for PDI, 13.1 ± 8.8% (n = 61) for giantin, and 59.4 ± 6.2% (n = 94) for LysoTracker.

degradation of the pre-TCR resulting in the attenuation of signaling. Such a sequence of events should be reflected in differences of stability in the plasma membrane of the pre-TCR versus αβTCR or γδTCR. This hypothesis was tested by cell surface labeling with biotin and immunoprecipitation with either anti-TCRβ or anti-TCRδ mAbs of cell lysates after a 2-h chase in culture. The pre-TCR and γδTCR turnover could be analyzed in the same cellular

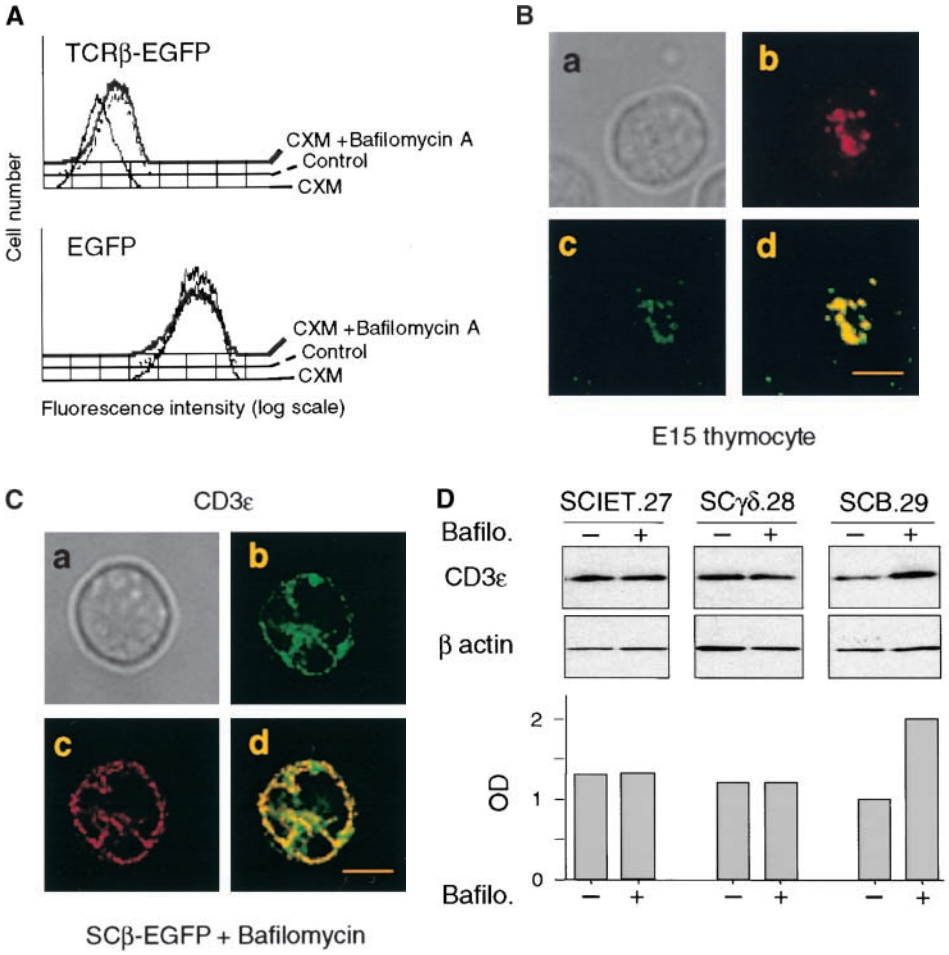

Figure 2. Localization of the pre-TCR in lysosomes in embryonic thymocytes and targeting of CD3 to lysosomes by the pre-TCR. (A) FACS® profile for green fluorescence of SCβ-EGFP and SC-EGFP cells upon treatment for 2 h with DMSO (control), cycloheximide and DMSO (CXM), and cycloheximide and bafilomycin A1 (CXM + Bafilomycin). (B, a) Phase-contrast image of E15 thymocyte, (b) staining with TCRβ mAb in red, (c) LAMP 2 mAb in green, and (d) merged images. 10–20% cells per thymocyte preparation were positive and displayed comparable patterns. 50 *z*-series optical sections were captured at 0.2-μm intervals. Bar, 10 μm. (C) SCβ-EGFP cells were treated with bafilomycin A1 for 6 h, permeabilized, and stained with CD3ε mAb followed by anti–hamster Ig immunoglobulins coupled to TRITC. A single section of one cell is displayed. Images of multiple cells showing comparable patterns are provided as supplemental material (see Figure S2, available at http://www.jem.org/cgi/content/full/jem.20020047/DC1. (a) Phase-contrast image, (b) TCRβ-EGFP, (c) CD3ε, and (d) merged images. Bar, 10 μm. (D) Immunoblot analysis of the indicated cell lines with CD3ε and β actin antibodies after a 6-h treatment with DMSO or bafilomycin A1. Relative densitometric analysis is displayed.

environment, i.e., in the SCB.29 and SCγδ.28 cell lines. Because the expression of both the pre-TCR and αβTCR in SCIET.27 cells transfected with rearranged TCRβ and TCRα genes could induce αβTCR activation in *trans*, αβTCR turnover was analyzed in the thymoma M14T (39) and T cell hybridoma B6.2.16 (38). Two-dimensional nonreduced versus reduced SDS-PAGE revealed that 88 ± 6% ($n = 3$) of the biotinylated pre-TCR detected immediately after labeling was lost after a 2-h chase and replaced by unlabeled, de novo–synthesized pre-TCRs as detected by coprecipitation of the same amount of CD3ε chains as revealed by immunoblot (Fig. 3 A). In contrast, the same analysis performed on both αβTCR- and γδTCR-expressing cell lines revealed no significant differences in the recoveries of labeled TCRs after a 2-h chase (Fig. 3, B–E). These results show that the pre-TCR has a turnover that is accelerated when compared with that of the αβTCR and γδTCR.

Pre-TCR Degradation Requires Dynamin and Actin Polymerization. Dynamin is essential in many intracellular trafficking events (47). The GTPase activity of dynamin was shown to be involved in clathrin-mediated endocytosis (41, 48) and caveolae internalization (49, 50). Recently, clathrin-independent endocytosis of the IL-2 receptor associated with rafts was also shown to depend on dynamin (51). We tested the involvement of dynamin in pre-TCR endocytosis by the transduction of SCB.29 cells with bicistronic retroviral vectors encoding EGFP and HA-tagged wild-type dynamin or dominant-negative K44A mutant (41). EGFP-positive cells were sorted and the expression of dynamin was checked in Western blots with HA antibodies. Immunoprecipitation from transduced SCB.29 cells that were kept for 2 h in culture after biotinylation revealed the prolonged stability of pre-TCR chains in cells expressing the K44A mutant dynamin compared with cells transduced with wild-type dynamin (Fig. 4, A–C). This suggests that the GTPase activity of dynamin is required for pre-TCR endocytosis. The actin cytoskeleton was hypothesized to be involved at various stages of the endocytic process from the spatial organization of the endocytic machinery to the vesicle movement into the cytoplasm (52). Moreover, filamentous actin was shown to accumulate in raft patches of lymphoid cells (53). To analyze the possible role of the actin cytoskeleton in pre-TCR degradation, we treated SCB.29 cells with the drug latrunculin B to sequester monomeric actin. Fig. 4 D shows the immunoprecipitation of biotinylated CD3ε chains from SCB.29 cells after a 2-h chase in the presence of decreasing concentrations of the drug. Densitometric analysis of the immunoprecipitated bands demonstrated a dose-dependent inhibition of CD3ε chain degradation, which suggests a role of actin cytoskeleton in the turnover of the pre-TCR.

Tyrosine Kinase Activity of p56^{lck} Influences Pre-TCR Expression in the Plasma Membrane. To test whether proximal pre-TCR signaling influenced the level of pre-TCR expression in the plasma membrane, we treated SCB.29 cells and embryonic day 15 FTOCs with the tyrosine kinase inhibitor PP2, which strongly and selectively inhibits p56^{lck} and p59^{fyn} (54). Immunoprecipitation of biotinylated CD3ε chains from SCB.29 cells treated with 10 μM PP2 during the 2-h chase in culture revealed the increased stability of CD3ε (Fig. 5 A). FACS® analysis of PP2-treated SCB.29 cells showed that pre-TCR expression was increased

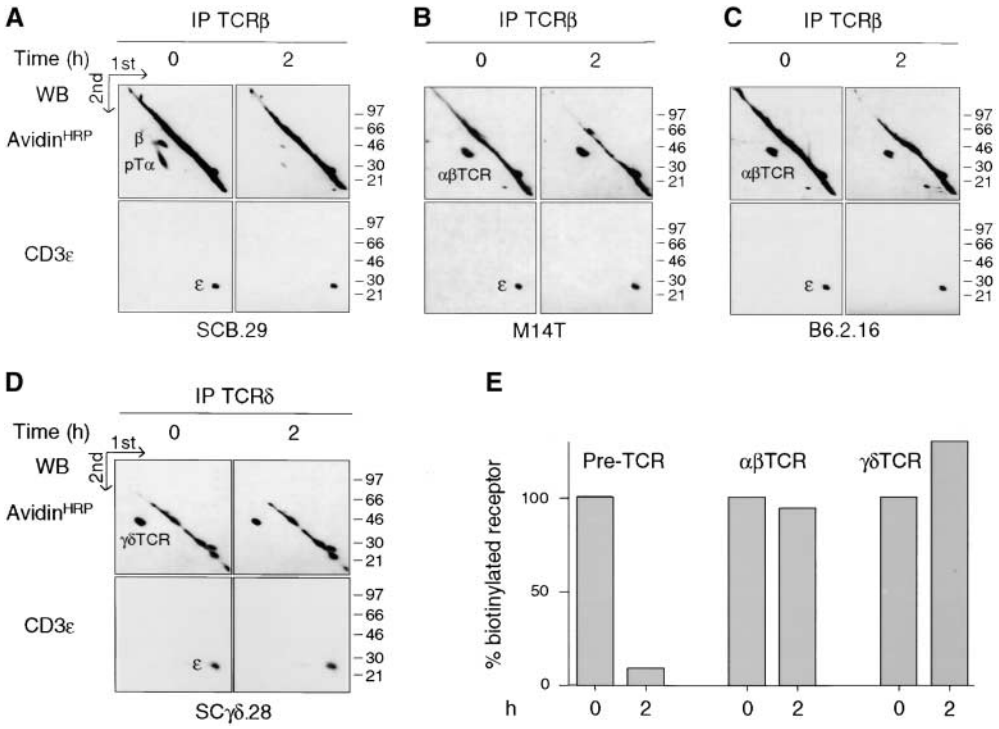

Figure 3. Limited stability of the pre-TCR in the plasma membrane. (A–D) Immunoprecipitation with the indicated antibody of the cell line defined at the bottom of each quadrant. Cells were labeled at the surface with biotin, lysed in 1% Brij 96, and immunoprecipitates were resolved by two-dimensional nonreduced versus reduced SDS-PAGE. Western blots with avidin-HRP and CD3ε antibodies on stripped membranes of immunoprecipitations performed immediately after labeling (0) and a 2-h chase in culture (2) are shown. IP, immunoprecipitation; WB, Western blots. (E) Densitometric analysis of the displayed experiment (the mean of the values obtained with the two cell lines is plotted for αβTCR).

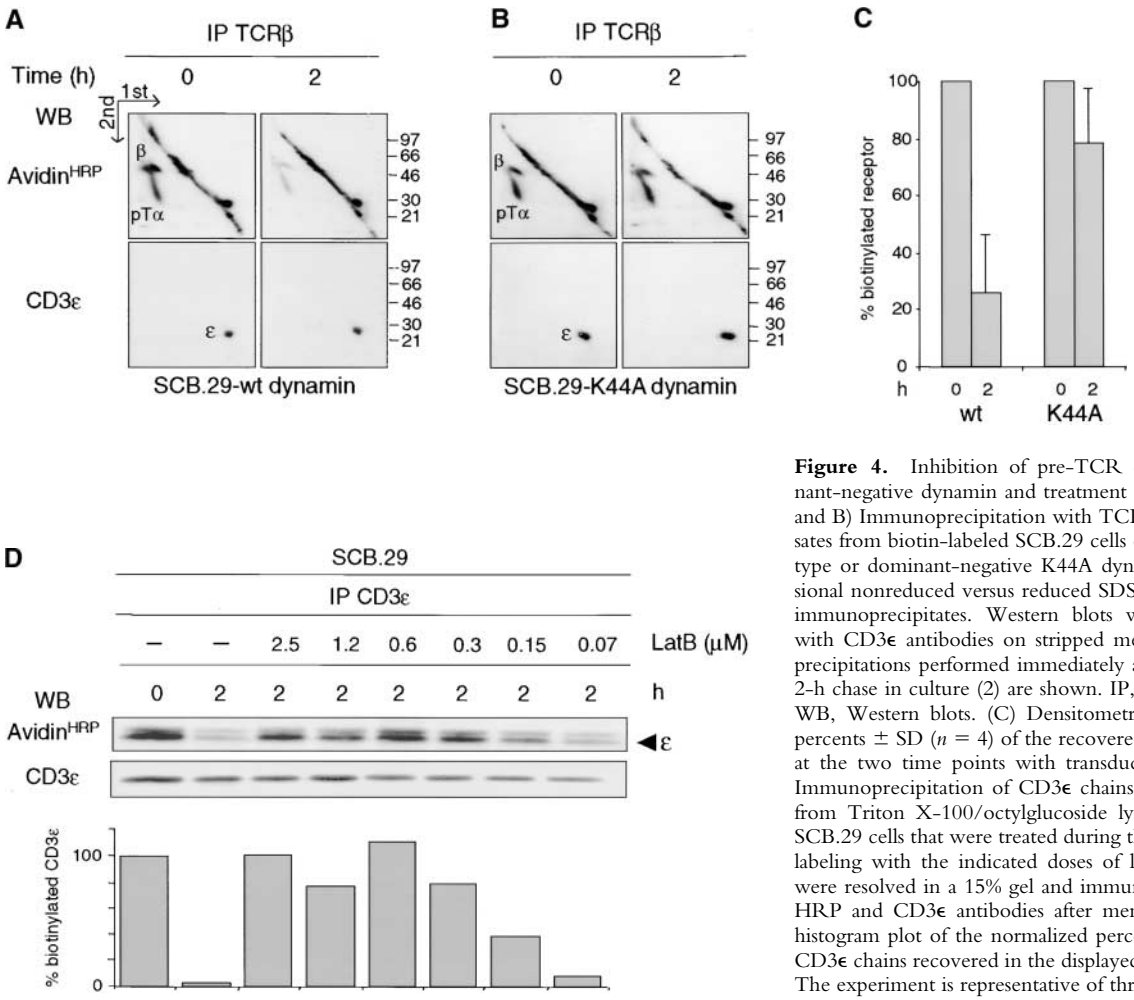

Figure 4. Inhibition of pre-TCR degradation by dominant-negative dynamin and treatment with latrunculin B. (A and B) Immunoprecipitation with TCRβ mAb of Brij 96 lysates from biotin-labeled SCB.29 cells expressing either wild-type or dominant-negative K44A dynamin and two-dimensional nonreduced versus reduced SDS-PAGE analysis of the immunoprecipitates. Western blots with avidin-HRP and with CD3ϵ antibodies on stripped membranes of immunoprecipitations performed immediately after labeling (0) and a 2-h chase in culture (2) are shown. IP, immunoprecipitation; WB, Western blots. (C) Densitometric analysis with mean percents ± SD ($n = 4$) of the recovered biotinylated receptor at the two time points with transduced SCB.29 cells. (D) Immunoprecipitation of CD3ϵ chains with 145-2C11 mAb from Triton X-100/octylglucoside lysates of biotin-labeled SCB.29 cells that were treated during the 2-h chase time after labeling with the indicated doses of latrunculin B. Samples were resolved in a 15% gel and immunoblotted with avidin-HRP and CD3ϵ antibodies after membrane stripping. The histogram plot of the normalized percentages of biotinylated CD3ϵ chains recovered in the displayed experiment is shown. The experiment is representative of three independent assays.

whereas CD8, which is also targeted to rafts (55), was not affected by this treatment (unpublished data). On day 15, FTOC PP2 treatment impaired the down-regulation of CD25, which is characteristic of pre-TCR–driven differentiation and resulted in higher levels of pre-TCR expression. No difference was observed with regard to γδTCR expression (Fig. 5 B). These results suggest that $p56^{lck}$ and possibly $p59^{fyn}$ activation results in an increased turnover of the pre-TCR in the plasma membrane.

Reduced Pre-TCR Turnover by Proteasome Inhibition. Ligation of the αβTCR was shown to induce ubiquitination as well as targeting to lysosomes of the associated CD3/ζ chains (56, 57, 23). On the other hand, inhibition of the proteasome was reported to result in the stabilization of the ligated αβTCR at the cell surface (25). Because the pre-TCR seems to promote, in a ligand-independent fashion, the same proximal signaling events that occur upon ligation of the αβTCR, we tested whether epoxomicin, a cell permeable as well as a selective and irreversible inhibitor of the proteasome (58), had any effect on the stability of the surface-labeled pre-TCR. Incubation of SCB.29 cells with epoxomicin resulted in a 75% inhibition of degradation of biotinylated pre-TCR proteins as detected in a 2-h chase after biotinylation (Fig. 6 A). The same effect was observed upon treatment with clastolactacystin β lactone, another inhibitor of the proteasome (see Figure S3 available at http://www.jem.org/cgi/content/full/jem.20020047/DC1). These results show that proteasome activity is involved in the ligand-independent degradation of the pre-TCR. Immunoprecipitation with TCRβ-specific antibodies followed by the dissociation of the immunocomplexes and reprecipitation with CD3ϵ-specific antibodies showed that surface biotinylated CD3ϵ chains that were associated with the pre-TCR were comparably degraded during the chase period and that degradation was likewise sensitive to epoxomicin (Fig. 6 B). In prothymocytes, ζ chains are associated with the pre-TCR and critically contribute to pre-TCR signaling (59). However, ζ chains can also be expressed independently of CD3ε chains in immature thymocytes and are only partially recruited during signaling by the pre-TCR (60). Therefore, we tested the stability of these pre-TCR independent ζ chains in the plasma membrane of SCB.29 cells by depleting SCB.29 cell lysates through TCRβ-specific immunoprecipitation and analyzing the remaining biotinylated ζ chains. The result revealed no

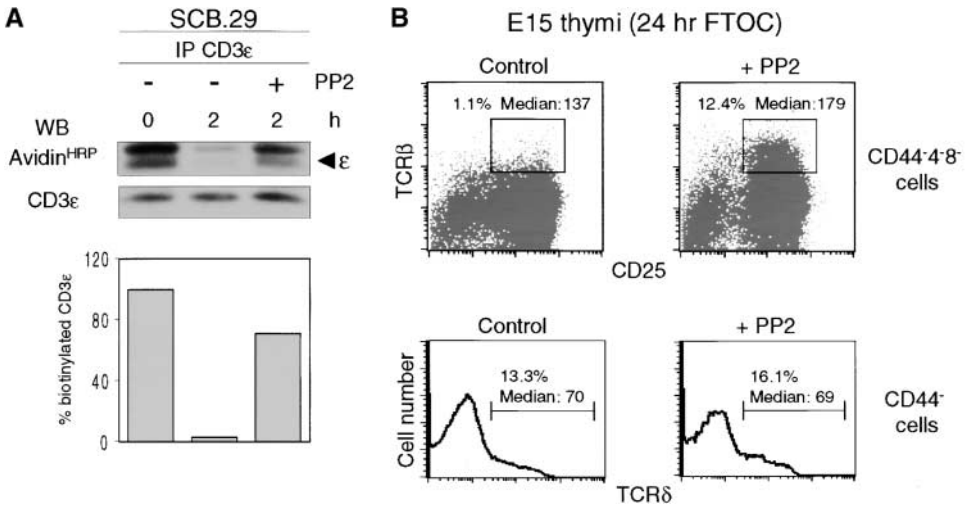

Figure 5. Reduced turnover and enhanced expression of the pre-TCR upon the inhibition of $p56^{lck}$ tyrosine kinase activity. (A) Immunoprecipitation of CD3ε chains with 145-2C11 mAb from Brij 96 lysates of biotin-labeled SCB.29 cells that were treated during the 2-h chase time after labeling with DMSO (−) or 10 μM PP2 (+). Samples were resolved in a 15% gel and immunoblotted with avidin-HRP and CD3ϵ antibodies after membrane stripping. The histogram plot of the normalized percentages of biotinylated CD3ϵ chains recovered in the displayed experiment is shown. The experiment is representative of four independent assays. (B) FACS® analysis of E15 24-h FTOC in the presence of DMSO (control) or 10 μM PP2 (+). The indicated cell subpopulations were electronically gated and analyzed for TCRβ versus CD25 and TCRδ expression. Relative representations of the selected cell fractions with respective median fluorescence intensities are displayed.

significant differences in the amount of biotinylated ζ chains recovered after the 2-h chase (Fig. 6 C), which implies that pre-TCR–independent ζ chains are relatively stable in the plasma membrane of SCB.29 cells and that a significant fraction of ζ chains on the cell surface are not internalized with the pre-TCR. These results suggest that pre-TCR–associated signal transducing molecules are selectively degraded.

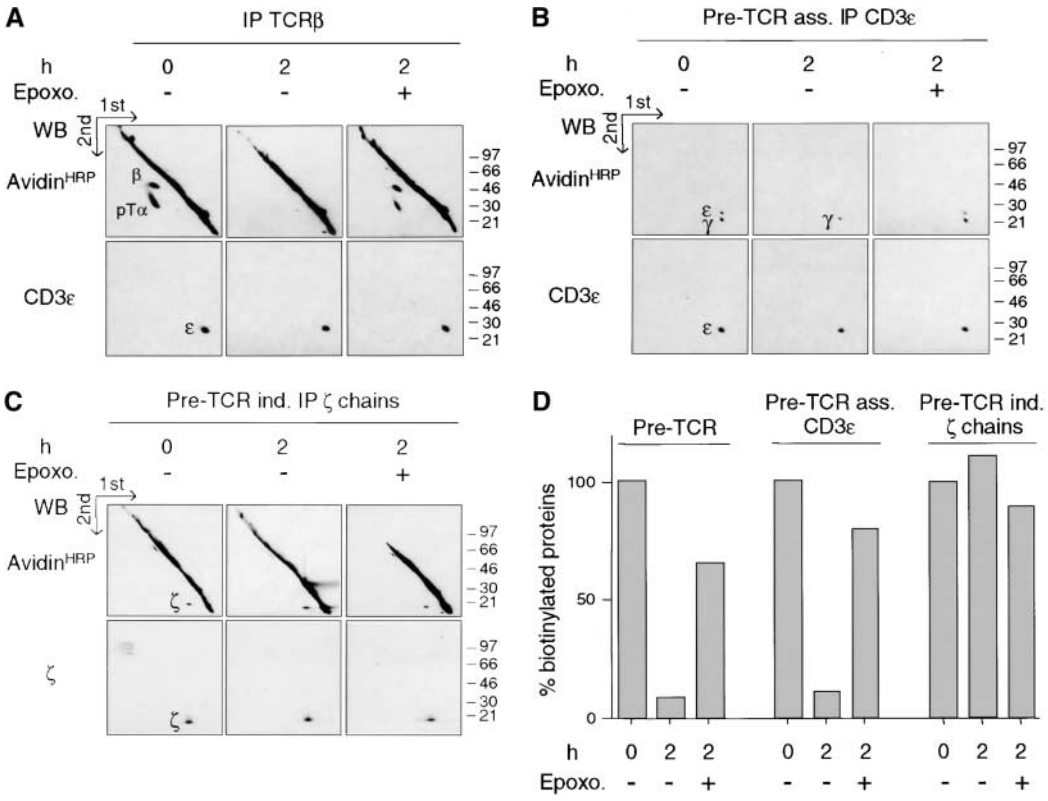

Figure 6. Reduction of the pre-TCR turnover by proteasome inhibition. (A) Immunoprecipitation with TCRβ mAb of SCB.29 cells lysed in 1% Brij 96 immediately after surface labeling with biotin (0) or a 2-h chase in the presence of DMSO (−) or epoxomicin (+). Two-dimensional nonreduced versus reduced gels were revealed in Western blots with avidin-HRP and after stripping with CD3ϵ antibodies. (B) Immunoprecipitation with 145-2C11 mAb of pre-TCR–associated CD3 chains as described in Materials and Methods. Two-dimensional nonreduced versus reduced gels were revealed as previously described. (C) Immunoprecipitation with G3 mAb of pre-TCR–independent ζ chains. After Western blots with avidin-HRP, membranes were stripped and revealed with anti–ζ chain rabbit serum. IP, immunoprecipitation; WB, Western Blots. (D) Densitometric analyses of the biotinylated pre-TCR chains, pre-TCR–associated CD3ϵ chains, and pre-TCR–independent ζ chains recovered at the indicated times and in the presence of the indicated treatment (means of at least two experiments are plotted).

Role of c-Cbl Ubiquitin Ligase Domain in the Regulation of Pre-TCR Turnover. c-Cbl was shown to bind to the SH3 domains of $p56^{lck}$ and $p59^{fyn}$ (61), as well as to phosphorylated ZAP-70 by its unique tyrosine kinase-binding domain (62, 63). The pre-TCR–dependent recruitment and phosphorylation of ZAP-70 in the plasma membrane of SCB.29 cells (17) could contribute to the twofold increase in tyrosine phosphorylation of c-Cbl in pre-TCR–expressing SCB.29 versus γδTCR-expressing SCγδ.28 cells (Fig. 7 A). The same level of c-Cbl phosphorylation as found in SCB.29 cells was obtained in SCγδ.28 after the cross-linking of the γδTCR with anti-TCRδ mAbs. Subcellular fractionation experiments revealed the selective enrichment of c-Cbl in the plasma membrane and the partition to rafts in SCB.29 cells, although c-Cbl was mostly confined to the Triton X-100 soluble fractions in both receptor-negative SCIET.27 and γδTCR-expressing SCγδ.28 cells (Fig. 7 B). These results suggest that c-Cbl is specifically recruited and activated into rafts during pre-TCR signaling. The RING finger domain of c-Cbl functions as an ubiquitin protein ligase (64) and tyrosine phosphorylation at a site flanking such RING finger enables

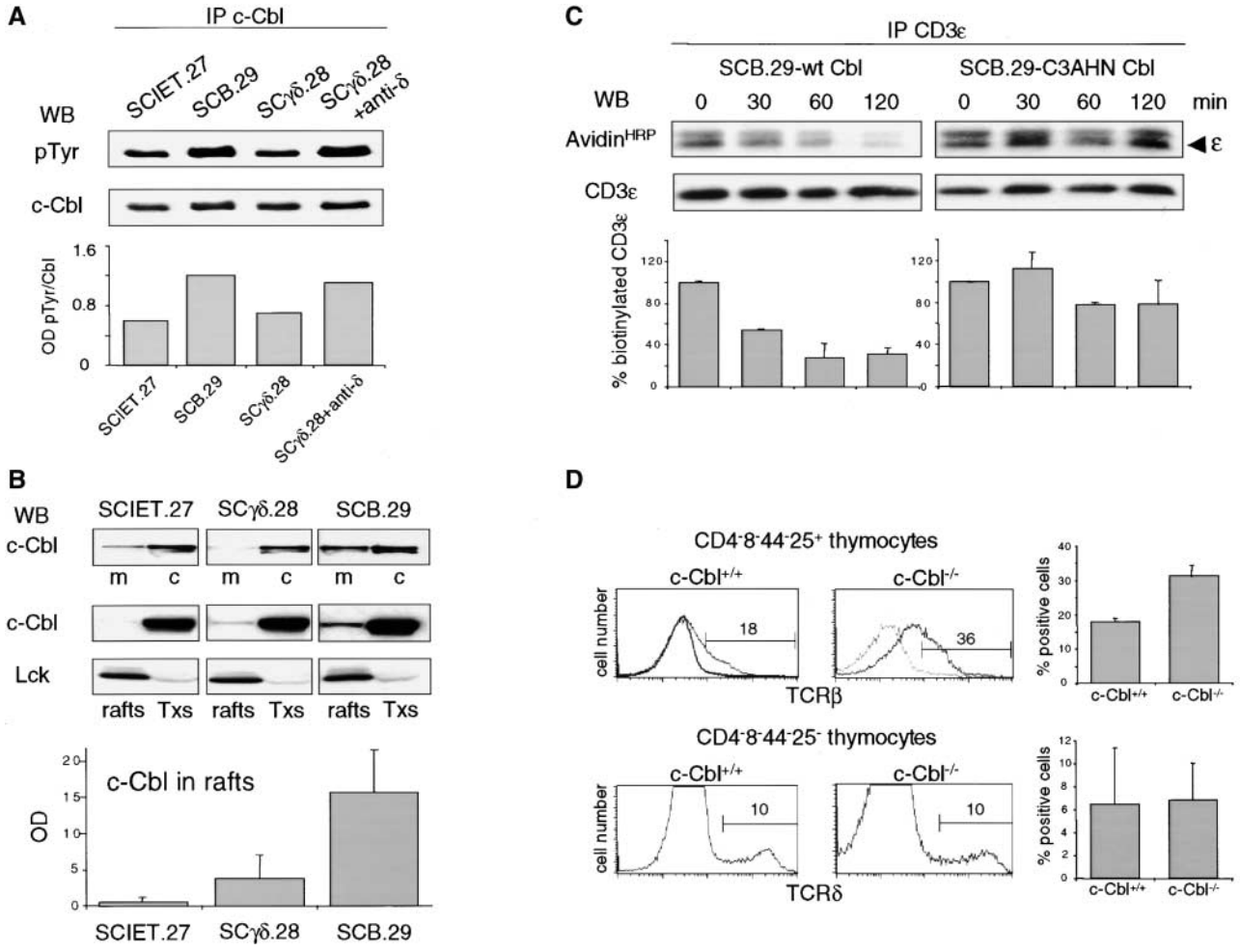

Figure 7. Translocation of c-Cbl to rafts in pre-TCR–expressing cells and regulation of pre-TCR expression by c-Cbl. (A) Analyses by immunoblot with antiphosphotyrosine mAb and anti-Cbl serum of c-Cbl immunoprecipitated from Triton X-100/octylglucoside lysates of the indicated cell lines. Relative densitometric analysis is displayed. (B) Immunoblot with Cbl serum of particulate (m) and soluble (c) fractions from lysates of the indicated cell lines (top), and the same analysis on rafts and Triton X-100 soluble (Txs) fractions from sucrose gradients loaded with lysates from the indicated cell lines. After c-Cbl immunoblot, membranes were stripped and probed with anti-$p56^{lck}$ immunoglobulins as a control of fractionations (bottom). Densitometric analyses of c-Cbl detected in rafts fractions of the indicated cell lines. Mean values ± SD of three independent experiments are plotted. (C) Immunoprecipitation of CD3ε chains with 145-2C11 mAb from Triton X-100/octylglucoside lysates of biotin-labeled SCB.29 cells expressing either wild-type or dominant-negative c-Cbl at the indicated times after labeling. Samples were resolved in a 15% gel and immunoblotted with avidin-HRP and CD3ε immunoglobulins after membrane stripping. The histogram plot of the normalized percents ± SD of biotinylated CD3ε chains recovered in two independent experiments is shown. (D) FACS® analysis of pre-TCR and γδTCR expression on the surface of purified $CD4^-8^-$ thymocytes that were further electronically gated with CD4, CD8, CD44, and CD25 antibodies with different fluorochromes. Pre-TCR and γδTCR expression on $CD44^-4^-8^-CD25^+$ and $CD44^-4^-8^-CD25^-$ thymocytes, respectively, from $c\text{-}Cbl^{+/+}$ and $c\text{-}Cbl^{-/-}$ C57BL/6 mice were detected by biotinylated TCRβ and TCRγδ mAbs revealed by streptavidin labeled with PBXL-3. In TCRβ histogram gray line represents the background fluorescence of an isotype-matched biotinylated negative mAb revealed by PBXL-3. Mean percents ± SD of pre-TCR and γδTCR-positive cells recovered from six and three mice, respectively, are plotted.

growth factor–dependent ubiquitination and degradation of tyrosine kinase receptors (65). To analyze the role of the c-Cbl ubiquitin ligase domain in pre-TCR down-regulation, we transduced SCB.29 cells with bicistronic retroviral vectors encoding EGFP and either wild-type c-Cbl or a dominant-negative RING finger mutant of c-Cbl with cysteines 396, 401, and 404 mutated to alanine, and histidine 398 to asparagine (C3AHN; reference 42). Surface labeling with biotin of transduced SCB.29 cells and immunoprecipitations of CD3ε chains at different times of chase showed the sustained recovery of biotinylated CD3ε chains in cells transduced with the dominant-negative C3AHN c-Cbl with respect to cells transduced with the wild-type c-Cbl (Fig. 7 C). This result demonstrated that an intact c-Cbl RING domain regulates the constitutive degradation of the pre-TCR–CD3 complex. The role of c-Cbl in the control of pre-TCR turnover was further demonstrated by the increased pre-TCR expression on the cell surface of $CD44^-4^-8^-CD25^+$ thymocytes from c-Cbl–deficient mice, whereas γδTCR expression was unaltered in $CD44^-4^-8^-CD25^-$ thymocytes from the same mice (Fig. 7 D).

Discussion

The pre-TCR plays a critical role in thymus development and determines the major wave of thymocyte proliferation during T cell development through signaling that apparently does not depend on interaction with exogenous ligands (16, 17). Cell-autonomous signaling by the pre-TCR is likely conferred to immature thymocytes by the expression in the plasma membrane of the pTα chain covalently linked to the rearranged TCRβ chain because the exit from the ER/cis-Golgi was shown to be required for pre-TCR signaling in the mouse (15). The pre-TCR is expressed at barely detectable levels on the surface of immature thymocytes. In human thymocytes this low expression was proposed to be dependent on a reduced transport to the plasma membrane determined by an ER retention motif present in the cytoplasmic tail of the human pTα chain (66). We could not detect an accumulation of the murine pre-TCR in the ER although we could localize the intracellular pre-TCR predominantly in the endosomal/lysosomal compartment. The observed endocytosis and degradation of the pre-TCR suggests that attenuation of the cell-autonomous signaling could be an important feature of pre-TCR signaling. In fact, the overexpression of pTα was shown to inhibit normal thymocyte differentiation (67).

Recently, the IL-2 receptor was shown to be translocated into rafts and internalized upon IL-2 binding by a clathrin-independent endocytic pathway through detergent-resistant structures (51). Moreover, the sorting of the IL-2 receptor to late endocytic compartments was shown to depend on ubiquitination (68). The pre-TCR is likely internalized by the same mechanism. The disruption of detergent-resistant plasma membrane domains by cholesterol extraction abolished pre-TCR signaling (17) and degradation (unpublished data). Polymerized actin accumulates in rafts patches (53) and the actin cytoskeleton was hypothesized to be involved in different steps of the endocytic process, like membrane invagination and fission as well as vesicle movement in the cytoplasm (52). We tested whether sequestration of monomeric actin by the drug latrunculin B had any effect on pre-TCR endocytosis. We found that exposure of the pre-TCR–expressing cell line SCB.29 to latrunculin B resulted in a dose-dependent inhibition of pre-TCR degradation (Fig. 4 D), thus implying the involvement of the actin cytoskeleton in sorting the pre-TCR to lysosomes.

The product of the protooncogene *c-cbl* was shown to be involved in the down-regulation of a number of growth factor receptors and is phosphorylated after αβTCR stimulation (69). We have previously shown that c-Cbl is constitutively phosphorylated in pre-TCR–expressing cells and activated in recombinase-deficient thymocytes upon anti-CD3 treatment (60). It was proposed that the phosphorylation and recruitment of c-Cbl by both Src family kinases and ZAP-70/Syk could negatively regulate the signaling of activated immune receptors through ubiquitin-dependent endocytosis or postendocytic sorting to lysosomes (70). Accordingly, activated T cells display ubiquitinated CD3 and ζ chains (56, 57) at the same time they are targeted to lysosomes (23), and c-Cbl–deficient mice display elevated CD3 expression on the cell surface of thymocytes (43). Indeed, pre-TCR expression in the plasma membrane of $CD44^-4^-8^-CD25^+$ thymocytes from such mice was also increased (Fig. 7 D). In SCB.29 cells p21 and p23, phosphorylated ζ chains were detected in association with ZAP-70 after long exposure of immunoblots revealed with antiphosphotyrosine mAbs, which represent an extremely sensitive reagent (59 and unpublished data). The lack of detection of ζ chains with antiubiquitin antibodies in SCB.29 cells could be related to high instability and poor association of such chains with the pre-TCR and/or the prevalence of monoubiquitinated forms (56) that are poorly recognized by the antisera.

A role of ubiquitination in regulating pre-TCR expression was implicated because of the observed stabilization of the pre-TCR after the inhibition of the proteasome. Inhibitors of both proteasome and lysosomes were shown to affect degradation of mammalian receptors that are ubiquitinated upon ligand stimulation. It was hypothesized that proteasome and lysosomes could be involved in the degradation of different parts of the molecules or that proteasome degradation of a nonreceptor protein might be required for targeting transport to the lysosomes (29). Recently, ubiquitin was shown to function as an internalization signal (26, 27) and in analogy to endocytosis mediated by clathrin-coated pits, which is limited by saturable components (71), it was shown to be rate-limiting for internalization (26). The accumulation of polyubiquitinated proteins during the treatment with proteasome inhibitors might interfere with the efficiency of receptor ubiquitination through the reduction of the pool of free ubiquitin (58, 72, 73). In this respect, we observed a 53 ± 10% (n =

4) reduction of free ubiquitin by immunoblot upon treatment of SCB.29 cells with 1 μM epoxomicin for 6 h (see Figure S4 available at http://www.jem.org/cgi/content/full/jem.20020047/DC1). The reduced turnover of the pre-TCR by the expression of the RING finger dominant-negative c-Cbl mutant suggests a critical role of ubiquitination by c-Cbl in signal attenuation not only by negatively regulating the intracellular effectors of the signaling machinery (42, 68, 74–77), but by determining the down-regulation of the pre-TCR itself. Furthermore, it was recently shown that c-Cbl associated to activated receptor tyrosine kinases could regulate their internalization through the recruitment of endophilins, which are involved in the induction of plasma membrane invagination in the early phases of endocytosis (78–79). Because c-Cbl is selectively recruited to the plasma membrane by the pre-TCR, it could also promote the endocytosis of pre-TCR–containing rafts by this function.

Constitutive signaling by the pre-TCR induces the increase in cytosolic Ca^{2+} and the activation of nuclear factor κB and nuclear factor of activated T cells (80). It is of interest to note that the function of the pre-TCR at the DN stage of thymocyte development cannot be replaced efficiently by the αβTCR. The early expression of an αβTCR leads to an inhibition of αβ T cell development and the generation of $CD4^-8^-$ thymocytes that express an αβTCR on the cell surface but do not or only inefficiently proceed along the αβ pathway (81–83). Thus, it is likely that the cell-autonomous signaling and endocytosis of the pre-TCR are both required for effective αβ T cell development, whereas the mere expression of an αβTCR or γδTCR diverts cells to a different lineage fate by different signals. Pre-TCR signal extinction by endocytosis and degradation may represent an important aspect of pre-TCR function as transgenic pTα overexpression resulted in the increased proliferation of DN3 cells and the apoptosis of DP thymocytes inhibiting αβ thymocyte development in a copy number–dependent fashion (67).

Regarding the latter observations, it was shown that a tumor-inhibitory mAb used in breast cancer immunotherapy can enhance the c-Cbl–mediated ubiquitination and degradation of the oncoprotein ErbB-2 expressed at the cell surface, suggesting that ubiquitination and degradation of receptor tyrosine kinases could be exploited for therapeutic purposes (84). Notch1-induced T cell leukemia in mice develops only in the presence of pre-TCR signaling, which suggests that deregulated expression of the pre-TCR in a particular genetic context can be tumorigenic (13, 14). Moreover, pTα chain expression was detected in all tested human acute T lymphoblastic leukemias (13). The c-Cbl–regulated proteolytic pathway described in this study could represent a potential therapeutic target in pre-TCR–dependent leukemia/lymphoma.

We thank Anja Siermann (Dana Farber Cancer Institute, Boston, MA) for technical assistance, Giuliana Gatti, Hans-Peter Hauri, Jeng-Shin Lee, and Elmar Jaeckel for antibodies and vectors, Larry Samelson for constant supply of rabbit anti–ζ chain antiserum, Monica Fabbri for dynamin plasmids and helpful discussions, and David Dunlap for the help and use of the Alembic facility (Dibit-HSR, Milano, Italy).

F. Grassi is a recipient of a Special Fellow Award of The Leukemia and Lymphoma Society.

Submitted: 10 January 2002
Revised: 9 April 2002
Accepted: 29 April 2002

References

1. Groettrup, M., K. Ungewiss, O. Azogui, R. Palacios, M.J. Owen, A.C. Hayday, and H. von Boehmer. 1993. A novel disulfide-linked heterodimer on pre-T cells consists of the T cell receptor β chain and a 33 kD glycoprotein. *Cell*. 75:283–294.
2. Haks, M.C., P. Krimpenfort, J. Borst, and A.M. Kruisbeek. 1998. The CD3γ chain is essential for development of both the TCRαβ and TCRγδ lineages. *EMBO J.* 17:1871–1882.
3. Malissen, M., A. Gillet, L. Ardouin, G. Bouvier, J. Trucy, P. Ferrier, E. Vivier, and B. Malissen. 1995. Altered T cell development in mice with a targeted mutation of the CD3ε gene. *EMBO J.* 14:4641–4653.
4. Malissen, M., A. Gillet, B. Rocha, J. Trucy, E. Vivier, C. Boyer, F. Kontgen, N. Brun, G. Mazza, E. Spanopoulou, et al. 1993. T cell development in mice lacking the CD3ζ/η gene. *EMBO J.* 12:4347–4355.
5. Liu, C.P., R. Ueda, J. She, J. Sancho, B. Wang, G. Weddell, J. Loring, C. Kurahara, E.C. Dudley, A. Hayday, et al. 1993. Abnormal T cell development in $CD3\zeta^{-/-}$ mutant mice and identification of a novel T cell population in the intestine. *EMBO J.* 12:4863–4875.
6. Ohno, H., T. Aoe, S. Taki, D. Kitamura, Y. Ishida, K. Rajewsky, and T. Saito. 1993. Developmental and functional impairment of T cells in mice lacking CD3ζ chains. *EMBO J.* 12:4357–4366.
7. Berger, M.A., V. Dave, M.R. Rhodes, G.C. Bosma, M.J. Bosma, D.J. Kappes, and D.L. Wiest. 1997. Subunit composition of pre-T cell receptor complexes expressed by primary thymocytes: CD3δ is physically associated but not functionally required. *J. Exp. Med.* 186:1461–1467.
8. Dave, V.P., Z. Cao, C. Browne, B. Alarcon, G. Fernandez-Miguel, J. Lafaille, A. de la Hera, S. Tonegawa, and D.J. Kappes. 1997. CD3δ deficiency arrests development of the αβ but not the γδ T cell lineage. *EMBO J.* 16:1360–1370.
9. Fehling, H.J., A. Krotkova, C. Saint-Ruf, and H. von Boehmer. 1995. Crucial role of the pre-T-cell receptor α gene in development of αβ but not γδ T cells. *Nature*. 375:795–798.
10. Fischer, A., and B. Malissen. 1998. Natural and engineered disorders of lymphocyte development. *Science*. 280:237–243.
11. Aifantis, I., J. Buer, H. von Boehmer, and O. Azogui. 1997. Essential role of the pre-T cell receptor in allelic exclusion of the T cell receptor β locus. *Immunity*. 7:601–607.
12. Ardouin, L., J. Ismaili, B. Malissen, and M. Malissen. 1998. The CD3γδε and CD3ζ/η modules are each essential for allelic exclusion at the T cell receptor β locus but are both dispensable for the initiation of V to (D)J recombination at the T cell receptor-β, -γ, and -δ loci. *J. Exp. Med.* 187:105–116.
13. Bellavia, D., A.F. Campese, S. Checquolo, A. Balestri, A. Biondi, G. Cazzaniga, U. Lendahl, H.J. Fehling, A.C. Hayday, L. Frati, et al. 2002. Combined expression of pTα and Notch3 in T cell leukemia identifies the requirement of

preTCR for leukemogenesis. *Proc. Natl. Acad. Sci. USA.* 99: 3788–3793.
14. Allman, D., F.G. Karnell, J.A. Punt, S. Bakkour, L. Xu, P. Myung, G.A. Koretzky, J.C. Pui, J.C. Aster, and W.S. Pear. 2001. Separation of Notch1 promoted lineage commitment and expansion/transformation in developing T cells. *J. Exp. Med.* 194:99–106.
15. O'Shea, C.C., A.P. Thornell, I.R. Rosewell, B. Hayes, and M.J. Owen. 1997. Exit of the pre-TCR from the ER/*cis*-Golgi is necessary for signaling differentiation, proliferation, and allelic exclusion in immature thymocytes. *Immunity.* 7:591–599.
16. Irving, B.A., F.W. Alt, and N. Killeen. 1998. Thymocyte development in the absence of pre-T cell receptor extracellular immunoglobulin domains. *Science.* 280:905–908.
17. Saint-Ruf, C., M. Panigada, O. Azogui, P. Debey, H. von Boehmer, and F. Grassi. 2000. Different initiation of pre-TCR and γδTCR signalling. *Nature.* 406:524–527.
18. Mellman, I. 1996. Endocytosis and molecular sorting. *Annu. Rev. Cell Dev. Biol.* 12:575–625.
19. Kirchhausen, T., J.S. Bonifacino, and H. Riezman. 1997. Linking cargo to vesicle formation: receptor tail interactions with coat proteins. *Curr. Opin. Cell Biol.* 9:488–495.
20. Letourneur, F., and R.D. Klausner. 1992. A novel di-leucine motif and a tyrosine-based motif independently mediate lysosomal targeting and endocytosis of CD3 chains. *Cell.* 69: 1143–1157.
21. Dietrich, J., J. Kastrup, B.L. Nielsen, N. Odum, and C. Geisler. 1997. Regulation and function of the CD3γ DxxxLL motif: a binding site for adaptor protein-1 and adaptor protein-2 in vitro. *J. Cell Biol.* 138:271–281.
22. Dietrich, J., T. Backstrom, J.P. Lauritsen, J. Kastrup, M.D. Christensen, F. von Bulow, E. Palmer, and C. Geisler. 1998. The phosphorylation state of CD3γ influences T cell responsiveness and controls T cell receptor cycling. *J. Biol. Chem.* 273:24232–24238.
23. Valitutti, S., S. Muller, M. Salio, and A. Lanzavecchia. 1997. Degradation of T cell receptor (TCR)–CD3-ζ complexes after antigenic stimulation. *J. Exp. Med.* 185:1859–1864.
24. D'Oro, U., M.S. Vacchio, A.M. Weissman, and J.D. Ashwell. 1997. Activation of the Lck tyrosine kinase targets cell surface T cell antigen receptors for lysosomal degradation. *Immunity.* 7:619–628.
25. Liu, H., M. Rhodes, D.L. Wiest, and D.A. Vignali. 2000. On the dynamics of TCR:CD3 complex cell surface expression and downmodulation. *Immunity.* 13:665–675.
26. Shih, S.C., K.E. Sloper-Mould, and L. Hicke. 2000. Monoubiquitin carries a novel internalization signal that is appended to activated receptors. *EMBO J.* 19:187–198.
27. Nakatsu, F., M. Sakuma, Y. Matsuo, H. Arase, S. Yamasaki, N. Nakamura, T. Saito, and H. Ohno. 2000. A di-leucine signal in the ubiquitin moiety. Possible involvement in ubiquitination-mediated endocytosis. *J. Biol. Chem.* 275:26213–26219.
28. Bonifacino, J.S., and A.M. Weissman. 1998. Ubiquitin and the control of protein fate in the secretory and endocytic pathways. *Annu. Rev. Cell Dev. Biol.* 14:19–57.
29. Hicke, L. 1999. Gettin' down with ubiquitin: turning off cell-surface receptors, transporters and channels. *Trends Cell Biol.* 9:107–112.
30. Langdon, W.Y., J.W. Hartley, S.P. Klinken, S.K. Ruscetti, and H.C. Morse III. 1989. v-cbl, an oncogene from a dual-recombinant murine retrovirus that induces early B-lineage lymphomas. *Proc. Natl. Acad. Sci. USA.* 86:1168–1172.
31. Levkowitz, G., H. Waterman, E. Zamir, Z. Kam, S. Oved, W.Y. Langdon, L. Beguinot, B. Geiger, and Y. Yarden. 1998. c-Cbl/Sli-1 regulates endocytic sorting and ubiquitination of the epidermal growth factor receptor. *Genes Dev.* 12: 3663–3674.
32. Lee, P.S., Y. Wang, M.G. Dominguez, Y.G. Yeung, M.A. Murphy, D.D. Bowtell, and E.R. Stanley. 1999. The Cbl protooncoprotein stimulates CSF-1 receptor multiubiquitination and endocytosis, and attenuates macrophage proliferation. *EMBO J.* 18:3616–3628.
33. Miyake, S., M.L. Lupher, B. Druker, and H. Band. 1998. The tyrosine kinase regulator Cbl enhances the ubiquitination and degradation of the platelet-derived growth factor receptor α. *Proc. Natl. Acad. Sci. USA.* 95:7927–7932.
34. Donovan, J.A., R.L. Wange, W.Y. Langdon, and L.E. Samelson. 1994. The protein product of the c-cbl protooncogene is the 120-kDa tyrosine-phosphorylated protein in Jurkat cells activated via the T cell antigen receptor. *J. Biol. Chem.* 269:22921–22924.
35. Linstedt, A.D., and H.P. Hauri. 1993. Giantin, a novel conserved Golgi membrane protein containing a cytoplasmic domain of at least 350 kDa. *Mol. Biol. Cell.* 4:679–693.
36. Itohara, S., N. Nakanishi, O. Kanagawa, R. Kubo, and S. Tonegawa. 1989. Monoclonal antibodies specific to native murine T-cell receptor γδ: analysis of γδ T cells during thymic ontogeny and in peripheral lymphoid organs. *Proc. Natl. Acad. Sci. USA.* 86:5094–5098.
37. van Oers, N.S., S.J. Teh, B.A. Irving, J. Tiong, A. Weiss, and H.S. Teh. 1994. Production and characterization of monoclonal antibodies specific for the murine T cell receptor ζ chain. *J. Immunol. Methods.* 170:261–268.
38. Groettrup, M., A. Baron, G. Griffiths, R. Palacios, and H. von Boehmer. 1992. T cell receptor (TCR) β chain homodimers on the surface of immature but not mature α, γ, δ chain deficient T cell lines. *EMBO J.* 11:2735–2745.
39. Primi, D., R.A. Clynes, E. Jouvin-Marche, J.P. Marolleau, E. Barbier, P.A. Cazenave, and K.B. Marcu. 1988. Rearrangement and expression of T cell receptor and immunoglobulin loci in immortalized $CD4^{-}CD8^{-}$ T cell lines. *Eur. J. Immunol.* 18:1101–1109.
40. Rebel, V.I., M. Tanaka, J.S. Lee, S. Hartnett, M. Pulsipher, D.G. Nathan, R.C. Mulligan, and C.A. Sieff. 1999. One-day ex vivo culture allows effective gene transfer into human nonobese diabetic/severe combined immune-deficient repopulating cells using high-titer vesicular stomatitis virus G protein pseudotyped retrovirus. *Blood.* 93:2217–2224.
41. Damke, H., T. Baba, D.E. Warnock, and S.L. Schmid. 1994. Induction of mutant dynamin specifically blocks endocytic coated vesicle formation. *J. Cell Biol.* 127:915–934.
42. Ota, S., K. Hazeki, N. Rao, M.L. Lupher, Jr., C.E. Andoniou, B. Druker, and H. Band. 2000. The RING finger domain of Cbl is essential for negative regulation of the Syk tyrosine kinase. *J. Biol. Chem.* 275:414–422.
43. Naramura, M., H.K. Kole, R.J. Hu, and H. Gu. 1998. Altered thymic positive selection and intracellular signals in Cbl-deficient mice. *Proc. Natl. Acad. Sci. USA.* 95:15547–15552.
44. Leca, G., S.E. Mansur, and A. Bensussan. 1995. Expression of VCAM-1 (CD106) by a subset of TCR γδ-bearing lymphocyte clones. Involvement of a metalloprotease in the specific hydrolytic release of the soluble isoform. *J. Immunol.* 154: 1069–1077.

45. Wiest, D.L., W.H. Burgess, D. McKean, K.P. Kearse, and A. Singer. 1995. The molecular chaperone calnexin is expressed on the surface of immature thymocytes in association with clonotype-independent CD3 complexes. *EMBO J.* 14:3425–3433.
46. Montixi, C., C. Langlet, A.M. Bernard, J. Thimonier, C. Dubois, M.A. Wurbel, J.P. Chauvin, M. Pierres, and H.T. He. 1998. Engagement of T cell receptor triggers its recruitment to low-density detergent-insoluble membrane domains. *EMBO J.* 17:5334–5348.
47. Schmid, S.L., M.A. McNiven, and P. De Camilli. 1998. Dynamin and its partners: a progress report. *Curr. Opin. Cell Biol.* 10:504–512.
48. Sweitzer, S.M., and J.E. Hinshaw. 1998. Dynamin undergoes a GTP-dependent conformational change causing vesiculation. *Cell.* 93:1021–1029.
49. Henley, J.R., E.W. Krueger, B.J. Oswald, and M.A. McNiven. 1998. Dynamin-mediated internalization of caveolae. *J. Cell Biol.* 141:85–99.
50. Oh, P., D.P. McIntosh, and J.E. Schnitzer. 1998. Dynamin at the neck of caveolae mediates their budding to form transport vesicles by GTP-driven fission from the plasma membrane of endothelium. *J. Cell Biol.* 141:101–114.
51. Lamaze, C., A. Dujeancourt, T. Baba, C.G. Lo, A. Benmerah, and A. Dautry-Varsat. 2001. Interleukin 2 receptors and detergent-resistant membrane domains define a clathrin-independent endocytic pathway. *Mol. Cell.* 7:661–671.
52. Qualmann, B., M.M. Kessels, and R.B. Kelly. 2000. Molecular links between endocytosis and the actin cytoskeleton. *J. Cell Biol.* 150:F111–F116.
53. Harder, T., and K. Simons. 1999. Clusters of glycolipid and glycosylphosphatidylinositol-anchored proteins in lymphoid cells: accumulation of actin regulated by local tyrosine phosphorylation. *Eur. J. Immunol.* 29:556–562.
54. Hanke, J.H., J.P. Gardner, R.L. Dow, P.S. Changelian, W.H. Brissette, E.J. Weringer, B.A. Pollok, and P.A. Connelly. 1996. Discovery of a novel, potent, and Src family-selective tyrosine kinase inhibitor. Study of Lck- and FynT-dependent T cell activation. *J. Biol. Chem.* 271:695–701.
55. Arcaro, A., C. Gregoire, N. Boucheron, S. Stotz, E. Palmer, B. Malissen, and I.F. Luescher. 2000. Essential role of CD8 palmitoylation in CD8 coreceptor function. *J. Immunol.* 165: 2068–2076.
56. Cenciarelli, C., D. Hou, K.C. Hsu, B.L. Rellahan, D.L. Wiest, H.T. Smith, V.A. Fried, and A.M. Weissman. 1992. Activation-induced ubiquitination of the T cell antigen receptor. *Science.* 257:795–797.
57. Hou, D., C. Cenciarelli, J.P. Jensen, H.B. Nguygen, and A.M. Weissman. 1994. Activation-dependent ubiquitination of a T cell antigen receptor subunit on multiple intracellular lysines. *J. Biol. Chem.* 269:14244–14247.
58. Meng, L., R. Mohan, B.H. Kwok, M. Elofsson, N. Sin, and C.M. Crews. 1999. Epoxomicin, a potent and selective proteasome inhibitor, exhibits in vivo antiinflammatory activity. *Proc. Natl. Acad. Sci. USA.* 96:10403–10408.
59. van Oers, N.S., H. von Boehmer, and A. Weiss. 1995. The pre-T cell receptor (TCR) complex is functionally coupled to the TCR-ζ subunit. *J. Exp. Med.* 182:1585–1590.
60. Grassi, F., E. Barbier, S. Porcellini, H. von Boehmer, and P.A. Cazenave. 1999. Surface expression and functional competence of CD3-independent TCR ζ-chains in immature thymocytes. *J. Immunol.* 162:2589–2596.
61. Fukazawa, T., K.A. Reedquist, T. Trub, S. Soltoff, G. Panchamoorthy, B. Druker, L. Cantley, S.E. Shoelson, and H. Band. 1995. The SH3 domain-binding T cell tyrosyl phosphoprotein p120. Demonstration of its identity with the c-cbl protooncogene product and in vivo complexes with Fyn, Grb2, and phosphatidylinositol 3-kinase. *J. Biol. Chem.* 270:19141–19150.
62. Lupher, M.L., K.A. Reedquist, S. Miyake, W.Y. Langdon, and H. Band. 1996. A novel phosphotyrosine-binding domain in the N-terminal transforming region of Cbl interacts directly and selectively with ZAP-70 in T cells. *J. Biol. Chem.* 271:24063–24068.
63. Meng, W., S. Sawasdikosol, S.J. Burakoff, and M.J. Eck. 1999. Structure of the amino-terminal domain of Cbl complexed to its binding site on ZAP-70 kinase. *Nature.* 398:84–90.
64. Joazeiro, C.A., S.S. Wing, H. Huang, J.D. Leverson, T. Hunter, and Y.C. Liu. 1999. The tyrosine kinase negative regulator c-Cbl as a RING-type, E2-dependent ubiquitin-protein ligase. *Science.* 286:309–312.
65. Levkowitz, G., H. Waterman, S.A. Ettenberg, M. Katz, A.Y. Tsygankov, I. Alroy, S. Lavi, K. Iwai, Y. Reiss, A. Ciechanover, et al. 1999. Ubiquitin ligase activity and tyrosine phosphorylation underlie suppression of growth factor signaling by c-Cbl/Sli-1. *Mol. Cell.* 4:1029–1040.
66. Carrasco, Y.R., A.R. Ramiro, C. Trigueros, V.G. de Yebenes, M. Garcia-Peydro, and M.L. Toribio. 2001. An endoplasmic reticulum retention function for the cytoplasmic tail of the human pre-T cell receptor (TCR) α chain: potential role in the regulation of cell surface pre-TCR expression levels. *J. Exp. Med.* 193:1045–1058.
67. Lacorazza, H.D., H.E. Porritt, and J. Nikolich-Zugich. 2001. Dysregulated expression of pre-Tα reveals the opposite effects of pre-TCR at successive stages of T cell development. *J. Immunol.* 167:5689–5696.
68. Rocca, A., C. Lamaze, A. Subtil, and A. Dautry-Varsat. 2001. Involvement of the ubiquitin/proteasome system in sorting of the interleukin 2 receptor β chain to late endocytic compartments. *Mol. Biol. Cell.* 12:1293–1301.
69. Thien, C.B., and W.Y. Langdon. 2001. Cbl: many adaptations to regulate protein tyrosine kinases. *Nat. Rev. Mol. Cell Biol.* 2:294–307.
70. Lupher, M.L., N. Rao, M.J. Eck, and H. Band. 1999. The Cbl protooncoprotein: a negative regulator of immune receptor signal transduction. *Immunol. Today.* 20:375–382.
71. Warren, R.A., F.A. Green, P.E. Stenberg, and C.A. Enns. 1998. Distinct saturable pathways for the endocytosis of different tyrosine motifs. *J. Biol. Chem.* 273:17056–17063.
72. Swaminathan, S., A.Y. Amerik, and M. Hochstrasser. 1999. The Doa4 deubiquitinating enzyme is required for ubiquitin homeostasis in yeast. *Mol. Biol. Cell.* 10:2583–2594.
73. Schubert, U., D.E. Ott, E.N. Chertova, R. Welker, U. Tessmer, M.F. Princiotta, J.R. Bennink, H.G. Krausslich, and J.W. Yewdell. 2000. Proteasome inhibition interferes with gag polyprotein processing, release, and maturation of HIV-1 and HIV-2. *Proc. Natl. Acad. Sci. USA.* 97:13057–13062.
74. Ota, Y., and L.E. Samelson. 1997. The product of the proto-oncogene c-cbl: a negative regulator of the Syk tyrosine kinase. *Science.* 276:418–420.
75. Lupher, M.L., Jr., N. Rao, N.L. Lill, C.E. Andoniou, S. Miyake, E.A. Clark, B. Druker, and H. Band. 1998. Cbl-mediated negative regulation of the Syk tyrosine kinase. A critical role for Cbl phosphotyrosine-binding domain binding to Syk phosphotyrosine 323. *J. Biol. Chem.* 273:35273–

35281.
76. Rao, N., M.L. Lupher, Jr., S. Ota, K.A. Reedquist, B.J. Druker, and H. Band. 2000. The linker phosphorylation site Tyr292 mediates the negative regulatory effect of Cbl on ZAP-70 in T cells. *J. Immunol.* 164:4616–4626.
77. Andoniou, C.E., N.L. Lill, C.B. Thien, M.L. Lupher, Jr., S. Ota, D.D. Bowtell, R.M. Scaife, W.Y. Langdon, and H. Band. 2000. The Cbl proto-oncogene product negatively regulates the Src-family tyrosine kinase Fyn by enhancing its degradation. *Mol. Cell. Biol.* 20:851–867.
78. Petrelli, A., G.F. Gilestro, S. Lanzardo, P.M. Comoglio, N. Migone, and S. Giordano. 2002. The endophilin-CIN85-Cbl complex mediates ligand-dependent downregulation of c-Met. *Nature.* 416:187–190.
79. Soubeyran, P., K. Kowanetz, I. Szymkiewicz, W.Y. Langdon, and I. Dikic. 2002. Cbl-CIN85-endophilin complex mediates ligand-induced downregulation of EGF receptors. *Nature.* 416:183–187.
80. Aifantis, I., F. Gounari, L. Scorrano, C. Borowski, and H. von Boehmer. 2001. Constitutive pre-TCR signaling promotes differentiation through Ca^{2+} mobilization and activation of NF-κB and NFAT. *Nat. Immunol.* 2:403–409.
81. Bruno, L., H.J. Fehling, and H. von Boehmer. 1996. The αβ T cell receptor can replace the γδ receptor in the development of γδ lineage cells. *Immunity.* 5:343–352.
82. Fritsch, M., A. Andersson, K. Petersson, and F. Ivars. 1998. A TCR α chain transgene induces maturation of $CD4^{-}8^{-}$ $\alpha\beta^{+}$ T cells from γδ T cell precursors. *Eur. J. Immunol.* 28:828–837.
83. Terrence, K., C.P. Pavlovich, E.O. Matechak, and B.J. Fowlkes. 2000. Premature expression of T cell receptor (TCR)αβ suppresses TCRγδ gene rearrangement but permits development of γδ lineage T cells. *J. Exp. Med.* 192: 537–548.
84. Klapper, L.N., H. Waterman, M. Sela, and Y. Yarden. 2000. Tumor-inhibitory antibodies to HER-2/ErbB-2 may act by recruiting c-Cbl and enhancing ubiquitination of HER-2. *Cancer Res.* 60:3384–3388.